HHS Public Access

Author manuscript

Nat Biotechnol. Author manuscript; available in PMC 2016 November 21.

Published in final edited form as:

Nat Biotechnol. 2015 February ; 33(2): 204–209. doi:10.1038/nbt.3124.

Optogenetics enables functional analysis of human embryonic stem cell–derived grafts in a Parkinson's disease model

Julius A Steinbeck[1,2], **Se Joon Choi**[3], **Ana Mrejeru**[3], **Yosif Ganat**[1,2], **Karl Deisseroth**[4,5,6], **David Sulzer**[3,7,8], **Eugene V Mosharov**[3], and **Lorenz Studer**[1,2]

[1]Center for Stem Cell Biology, Sloan-Kettering Institute for Cancer Research, New York, New York, USA

[2]Developmental Biology Program, Sloan-Kettering Institute for Cancer Research, New York, New York, USA

[3]Department of Neurology, Columbia University Medical Center, New York, New York, USA

[4]Department of Bioengineering, Stanford University, Stanford, California, USA

[5]Department of Psychiatry, Stanford University, Stanford, California, USA

[6]Howard Hughes Medical Institute, Stanford University, Stanford, California, USA

[7]Department of Psychiatry, Columbia University Medical Center, New York, New York, USA

[8]Department of Pharmacology, Columbia University Medical Center, New York, New York, USA

Abstract

Recent studies have shown evidence of behavioral recovery after transplantation of human pluripotent stem cell (PSC)-derived neural cells in animal models of neurological disease[1–4]. However, little is known about the mechanisms underlying graft function. Here we use optogenetics to modulate in real time electrophysiological and neurochemical properties of mesencephalic dopaminergic (mesDA) neurons derived from human embryonic stem cells (hESCs). In mice that had recovered from lesion-induced Parkinsonian motor deficits, light-induced selective silencing of graft activity rapidly and reversibly re-introduced the motor deficits. The re-introduction of motor deficits was prevented by the dopamine agonist apomorphine. These results suggest that functionality depends on graft neuronal activity and dopamine release. Combining optogenetics, slice electrophysiology and pharmacological approaches, we further

Correspondence should be addressed to L.S. (studerl@mskcc.org) or E.V.M. (em706@columbia.edu).

Note: Any Supplementary Information and Source Data files are available in the online version of the paper.

AUTHOR CONTRIBUTIONS

J.A.S.: conception and study design, hESC manipulation, differentiation and characterization, calcium imaging, animal lesioning and transplantation, histological and behavioral assays, data analysis and interpretation and writing of manuscript. S.J.C. and A.M.: slice physiology and data analysis, writing of manuscript. Y.G.: animal lesioning and transplantation assays. K.D.: study design and provision of materials. D.S.: study design and data interpretation.

E.V.M.: study design, neurochemical assays, data analysis and interpretation and writing of manuscript. L.S.: conception and study design, data analysis and interpretation, writing of manuscript.

COMPETING FINANCIAL INTERESTS

The authors declare competing financial interests: details are available in the online version of the paper.

show that mesDA-rich grafts modulate host glutamatergic synaptic transmission onto striatal medium spiny neurons in a manner reminiscent of endogenous mesDA neurons. Thus, application of optogenetics in cell therapy can link transplantation, animal behavior and postmortem analysis to enable the identification of mechanisms that drive recovery.

The therapeutic potential of human cells is commonly assessed using long-term behavioral assays after transplantation into a relevant animal model of neurological disease. Yet such experiments do not pinpoint the biological mechanisms responsible for behavioral recovery. In the central nervous system, transplanted cells may induce therapeutic benefits through a variety of mechanisms, such as the release of trophic factors, the induction of remyelination, immunomodulation or actual network repair. For Parkinson's disease therapy, it has been suggested that full behavioral recovery requires functional integration of grafted dopamine neurons into diseased host circuits[5,6]. However, the prospect of functional neuronal integration, also known as graft-mediated neuronal network repair, remains poorly validated owing to the lack of methods to selectively interfere with neuronal graft function. In previous studies the role of grafted cells has been assessed by selective ablation of the graft, using diphtheria toxin in a model of spinal cord injury[7] or chemical re-lesioning in an animal model of Parkinson's disease[5]. But these approaches lead to the complete elimination of the transplanted cells without addressing the specific mechanism of action. In contrast, optogenetics allows the reversible functional manipulation of genetically and spatially defined circuits with unprecedented precision[8]. Controlling the activity of specific neurons can link circuit activity to animal behavior in freely moving animals in real time[9], including animals with neurological disease[10,11]. Despite its transformative role in neuroscience, optogenetics had only limited impact on human stem cell biology[12,13], in part because human PSC-derived neurons initially exhibit immature functional properties[14] and may not form synapses efficiently across species boundaries in the adult or diseased brain. In principle, however, optogenetics is an ideal strategy for interrogating graft function and graft-to-host connectivity, with the potential to resolve long-standing mechanistic questions[15]. Ongoing work toward the first clinical use of hPSC-derived mesDA neurons in patients with Parkinson's disease further underscores the importance of gaining mechanistic insights into graft function and connectivity.

To dissect the functionality of mesDA neurons transplanted into the lesioned striatum[1–3], we transduced undifferentiated hESCs to express the inhibitory chloride pump halorhodopsin[8] eNpHR3.0-EYFP (called HALO) or EYFP alone under control of the human synapsin promoter. The synapsin promoter was selected for its strong expression and lack of silencing in PSC-derived mesDA neurons. The use of a pan-neuronal promoter mimics the most likely clinical scenario as neither fetal nor prospective PSC-derived grafts are composed exclusively of mesDA neurons. The resulting clonal hESC lines were validated for genomic integration of transgenes (Supplementary Fig. 1) and maintenance of pluripotent marker expression (Fig. 1a). Differentiation into hESC-derived mesDA neurons was done as described previously[2]. At day 20 of differentiation, we observed co-expression of the mesDA neuron markers LMX1A and FOXA2 in >90% of cells (Supplementary Fig. 2a,c) in both lines. Expression of the early postmitotic mesDA neuron marker NR4A2 (NURR1) was detected in about 50% of cells by day 30 in both HALO and EYFP clones (Supplementary

Fig. 2b,c). Robust expression of HALO and EYFP was observed by days 25–30 of differentiation. Only clones expressing the transgenes in >98% of all $TUJ1^+$ neurons (Fig. 1b,e) or $TH^+/NURR1^+$ neurons (Fig. 1c,e) were used for further experiments. HALO expression was mainly confined to the cell membrane and processes of $TH^+/NURR1^+$ neurons (Fig. 1d). For further phenotypic characterizations of the clones, see Supplementary Figure 3a–c.

To test the functionality of hESC-derived neurons *in vitro*, we incubated mature mesDA-rich cultures with the calcium dye Fura-2 and imaged them under continuous perfusion (Fig. 2a). Most cells with neuronal morphology showed a transient calcium increase after application of a 15-s pulse of 100 μM glutamate (Fig. 2b,c, and Supplementary Video 1) or 55 mM KCl (data not shown). To test HALO functionally in cultured neurons, we continuously perfused them with saline containing 50 μM glutamate (Fig. 2d) while intermittently exposing cultures to 30-s pulses of 550 nm (green) light (Fig. 2e and Supplementary Video 2). As expected, halorhodopsin activation induced an immediate decrease in the calcium response following every light pulse (Fig. 2f and Supplementary Fig. 4i). Corresponding bright field and EYFP fluorescent images are shown in Figure 2g,h. A similar response to glutamate was observed in control mesDA cultures expressing EYFP (Supplementary Fig. 4a–c and Supplementary Video 3), however, those cells showed no response to light exposure (Supplementary Fig. 4d–i and Supplementary Video 4).

We next tested whether optogenetic control of neuronal activity, as demonstrated by calcium imaging experiments, enables modulation of neurotransmitter release. For this purpose, supernatants of cells exposed to various extrinsic stimuli were collected and analyzed by reversed phase high-performance liquid chromatography (HPLC) with electrochemical detection. EYFP- or HALO-expressing neuronal cultures could be stimulated to release about twice the amount of dopamine (DA) following KCl or glutamate exposure compared to basal release (saline versus GLU; Sidak's multiple comparisons test, $t = 5.27$, $P < 0.0001$; Fig. 2i). Dopamine release from EYFP-expressing mesDA-rich cultures (black bars) was unchanged when illuminated for 10 min at 543 nm (saline versus saline + 543 and GLU versus GLU + 543). In contrast, HALO-expressing cultures (green bars) showed a significant reduction of dopamine release during 543 nm illumination (−55%, saline versus saline + 543, $t = 2.66$, $P < 0.05$). Similarly, optogenetic suppression of neuronal activity was sufficient to over-ride glutamate stimulation (−85%, GLU versus GLU + 543, $t = 8.50$, $P < 0.0001$).

After confirming optogenetic control over both physiological and neurochemical properties of hESC-derived mesDA neurons *in vitro*, we sought to test transplant functionality *in vivo*. For this purpose, adult (2–3 months old) immunodeficient mice (NOD-SCID IL2Rgc) were subjected to unilateral 6-hydroxydopamine (6-OHDA) lesions, as described previously[2]. Only animals with a strong behavioral phenotype of >6 ipsilateral rotations/min in response to amphetamine exposure were deemed hemiparkinsonian and selected for further experiments. At 3 weeks after lesioning, animals received 2×10^5 hESC-derived mesDA-rich cells (day 25, Nurr1 stage of differentiation[16]). Animals grafted with mesDA neurons from HALO or EYFP hESC clones recovered from amphetamine-induced rotational asymmetry over the course of 16 weeks in contrast to lesion-only animals (Fig. 3a).

Histological analysis confirmed the extent of the lesion, loss of endogenous mesDA neurons in the substantia nigra and the presence of TH^+ mesDA-rich grafts (Supplementary Fig. 5) at 4–6 months after transplantation, as described previously[2,17]. TH^+ innervation into the dorsolateral striatum was partially restored in grafted versus lesion-only control animals (Supplementary Fig. 5f). HALO- and EYFP-grafted animals showed comparable grafts at various stages after transplantation (Supplementary Fig. 6).

Acute brain slices from recovered animals at 4–6 months after transplantation were used for electrophysiology. Donor neurons could be clearly identified by virtue of their fluorescence and typical differential interference contrast (DIC) appearance and were analyzed in the whole-cell patch clamp configuration. HALO- (12/14) and EYFP-(14/15) expressing neurons had a resting membrane potential between −40 and −60 mV and produced the typical pacemaking activity of mesDA neurons[2,18] with firing frequencies of 1–4 Hz (Fig. 3b and Supplementary Fig. 7). In response to illumination, HALO-expressing neurons (7/7) showed an immediate additional hyperpolarization of −17 ± 2 mV and a cessation of action potential firing at a light intensity of 2 mW/mm^2 (Fig. 3b, upper trace); the firing pattern of EYFP-expressing neurons remained unchanged (Fig. 3b, lower trace). Next we tested the functional integration of grafted human neurons into host circuitry. Local electrical stimulation evoked excitatory post-synaptic currents in grafted, opsin-expressing human neurons ($n = 7$), which could be blocked by the AMPA receptor antagonist NBQX (−76.3 ± 10.4%, $n = 5$, Fig. 3c). This finding confirms that despite their ectopic location, human neurons grafted into the striatum received functional glutamatergic inputs from the host, as reported previously for grafted primary mouse dopaminergic neurons[19].

For the analysis of graft-to-host connectivity, recovered animals were implanted with a fiber optic cannula for light delivery to the graft in awake, freely moving animals. We chose the corridor test[20,21] for these experiments because behavioral results have been shown to correlate well with the extent of the lesion. Moreover, this test does not require injection of amphetamine. Amphetamine causes dopamine release by reverse transport, a process that is not affected by optogenetic graft silencing. For behavioral studies, amount of food intake was restricted and animals were habituated to the corridor for three consecutive days. Control animals (unlesioned and nongrafted, $n = 3$) explored the corridor and collected sucrose pellets from both sides equally, irrespective of graft illumination (Fig. 3d, blue bars, CTRL versus CTRL + 543 and Supplementary Video 5). Unilaterally lesioned animals before transplantation (LES., green and black bars, $n = 9$, Supplementary Video 6) showed a strong preference for pellet retrieval ipsilateral to the lesion. Injection of the dopamine-receptor-agonist apomorphine, which signals through lesion-sensitized dopamine receptors on medium spiny neurons (MSNs)[22,23] and striatal interneurons[22], resulted in an inversion of pellet retrieval behavior (green LES. bar + APO and Supplementary Video 7). This demonstrates the dopaminergic sensorimotor deficit and associated unilateral hypersensitivity of the basal ganglia circuitry. These lesioned animals, when grafted with HALO- or EYFP-expressing mesDA-rich cells showed a complete recovery in this behavioral test (HALO versus LES., $t = 6.27$, $P < 0.0001$; EYFP versus LES., $t = 3.83$, $P < 0.01$). Recovered animals with EYFP grafts ($n = 5$) showed no change in behavior under illumination (EYFP versus EYFP + 543, and Supplementary Video 8). In contrast, animals with HALO grafts ($n = 9$) demonstrated strong lateralized exploration and pellet retrieval

under optogenetic silencing (HALO versus HALO + 543, $t = 8.70$, $P < 0.0001$, Supplementary Video 9), which is reminiscent of and statistically not different from the behavior of severely lesioned animals (LES. versus HALO + 543, $t = 1.51$, $P = 0.64$). Similar results were obtained using spontaneous rotations as an independent behavioral assay (data not shown). These results strongly suggest that behavioral recovery from the Parkinsonian state is dependent on the activity of the graft. As these grafts do not exclusively contain dopamine neurons, we next sought to determine whether cessation of dopamine release is responsible for the observed reversion to disease-like behavior. For this purpose, animals with HALO-expressing grafts received an injection of the direct dopamine-receptor-agonist apomorphine before optogenetic testing ($n = 3$, HALO + 543 + APO). Under these conditions the animals did not revert to hemiparkinsonian behavior during optogenetic graft silencing (Supplementary Video 10), consistent with the idea that graft-released dopamine, now replaced by apomorphine, is the essential link between graft function and behavior. However, we cannot rule out that apomorphine, in addition to its well-documented effect on endogenous dopamine receptors of MSNs, could also affect other host or graft-derived neurons. It is also important to note that apomorphine injection in grafted animals did not produce the contralateral sensorimotor overshoot observed in lesioned animals (Fig. 3d, LES. + APO versus HALO + 543 + APO, $t = 4.81$, $P = 0.0002$). Therefore, the apomorphine data also indicate that the presence of the graft, regardless of whether it is silenced or not, can rescue maladaptive behaviors thought to be associated with basal ganglia hypersensitivity[24,25].

We next determined the anatomical and physiological correlates of the observed behavioral effects. Cortex and thalamus provide the main glutamatergic input for MSNs and therefore the basal ganglia loop that controls movement[26,27]. This excitatory input into MSNs is modulated by dopaminergic terminals emanating from the substantia nigra, which degenerate in Parkinson's disease[27–29]. Therefore, an ideal graft-to-host connectivity should involve modulation of glutamatergic inputs to MSNs in a manner similar to endogenous mesDA neurons. Histological analysis revealed robust fiber outgrowth into the host striatum. We observed human-specific synaptophysin alongside human axons[30] to co-localize with TH near the graft but also extending far into the dorsolateral striatum (Supplementary Fig. 8)[31]. In both HALO- and EYFP-grafted animals, confocal imaging showed human terminals in direct contact with dendrites and cell bodies of DARPP32$^+$ host MSNs (Fig. 3e,f and Supplementary Fig. 9), representing a morphological correlate of graft to host connectivity.

At the functional level, we first characterized the basic physiologic properties of MSNs in the vicinity of the graft. Resting membrane potential, rheobase, current-voltage relationship and firing frequency after current injection were not different between control, lesion-only and lesion + HALO groups (Supplementary Fig. 10). To test if mesDA-rich grafts could modulate host glutamatergic transmission onto MSNs, we electrically stimulated acute slices from behaviorally recovered and control animals at the corpus callosum while excitatory postsynaptic potentials (EPSPs) were recorded from MSNs near the graft. Corpus callosum stimulation activates not only glutamatergic but also other local terminals, producing an increase in extracellular dopamine that was absent in 6-OHDA lesion-only animals (Supplementary Fig. 11). Under these experimental conditions, normalized amplitudes of evoked EPSPs in MSNs from control (9/9 cells) and EYFP (7/7 cells) groups were

unchanged during illumination. In contrast, in 11 of 26 MSNs from animals with HALO grafts, optogenetic graft silencing resulted in significant reversible reduction in evoked EPSP amplitudes compared to either control animals or animals with EYFP grafts (Fig. 3g,h; CTRL + 560 versus HALO + 560, $t = 10.44$, $P < 0.0001$, and EYFP + 560 versus HALO + 560, $t = 8.61$, $P < 0.0001$). These data suggest that the graft could enhance EPSPs on host MSNs through the activation of D1 receptors, an effect inhibited by light-induced graft silencing. D1-dependent enhancement of AMPA EPSPs has been reported in several studies in cultured neurons[32–34] and in striatal slices[35–40]. In our experimental protocol, in which electrical stimulation in the nearby corpus callosum evokes repetitive dopamine release at 20-s intervals (Supplementary Fig. 11), the D1 antagonist SCH39166 (2 μM) decreased EPSP amplitudes in 6/7 MSNs from control animals (CTRL + 560 versus CTRL + D1 antagonist, $t = 10.40$, $P < 0.0001$) and in 4/6 MSNs from EYFP animals (EYFP + 560 versus EYFP + D1 antagonist, $t = 6.45$, $P < 0.0001$). There was, however, no effect of the D1 antagonist on EPSPs in lesion-only mice without transplanted neurons (Fig. 3i and Supplementary Fig. 12). The data thus are consistent with an ongoing D1 response that enhances EPSPs in MSNs under conditions in which dopamine is present following evoked stimulation. Previous studies in striatal slices emphasized the importance of D2 rather than D1 receptor–mediated modulation of MSNs[41]. However, direct optogenetic stimulation of endogenous D1+ MSNs *in vivo* has been shown to trigger behavioral recovery in 6-OHDA lesioned mice[11], consistent with our current data.

The magnitude and time frame of pharmacological D1 receptor inhibition and optogenetic graft silencing were identical (Fig. 3i), suggesting that in both cases reduced glutamatergic transmission could be mediated by the cessation of the excitatory action of dopamine released from the graft. However, our data do not rule out alternative mechanisms, such as the involvement of interneurons[41] or other indirect mechanisms, in mediating these neuromodulatory effects. Although future studies are needed to resolve remaining questions regarding detailed neurochemistry, the results clearly demonstrate that mesDA-rich grafts are capable of modulating glutamatergic synaptic transmission onto striatal MSNs. Our work also establishes the framework for follow-up studies using optogenetics to target specific neuron subtypes within mesDA-rich grafts. We propose that such experiments will help in refining the therapeutic efficacy and safety of this treatment strategy.

In conclusion, our study demonstrates the utility of optogenetics to dissect the mechanisms underlying hESC graft function in a preclinical model of Parkinson’s disease. Optogenetics is currently the only experimental strategy that achieves the spatial and temporal resolution required for the behavioral and physiological experiments presented. However, in future studies it may be interesting to integrate alternative technologies, such as DREADD-based strategies[42], that could enable long-term modulation of human graft function during graft maturation. Our results provide direct behavioral and physiologic evidence for the essential role of graft neuronal activity and connectivity in behavioral recovery. We further show that grafted hESC-derived mesDA neurons modulate glutamatergic transmission in the host striatum in a manner reminiscent of endogenous substantia nigra dopamine neurons. With a view toward the impending first clinical trials using PSC-derived mesDA neurons in Parkinson’s patients, our findings are encouraging as they indicate a possibility for network repair.

METHODS

Methods and any associated references are available in the online version of the paper.

ONLINE METHODS

Generation of stable opsin-expressing hESC lines

pLenti-*hSyn-eNpHR3.0-EYFP* (called HALO) and pLenti-*hSyn-EYFP* (called EYFP) vectors were provided by K.D. (http://www.stanford.edu/group/dlab/optogenetics/sequence_info.html). Lentivirus was produced via co-transfection of the HALO or EYFP plasmids with pUCMD.G and pCMVΔR8.91 into 293T cells, as previously described[43]. Lentivirus was 100× concentrated by ultracentrifugation at 100,000*g* for 90 min and stored at −80 °C. Passage 40 H9 human ES cells obtained from the MSKCC stem cell core facility were maintained as described previously[44], pretreated for 60 min with 10 μM ROCK inhibitor[45], dissociated to a single-cell suspension using Accutase (Life Technologies) and passed through a 40 μm mesh. 5×10^5 cells were incubated in 200 μl hESC media containing ROCK inhibitor with the addition of 10% high-titer lentiviral preparations in a tissue culture incubator for 6 h and resuspended by flicking the tube 1×/h. Then, cells were passed through a 40-μm mesh, counted and seeded on mouse embryonic fibroblasts (Globalstem) in hESC media with ROCK inhibitor at various densities ranging from 1 to 10^4 cells/cm^2. Ten days after plating, emerging colonies were picked and expanded before screening genomic DNA for integration of opsin and control transgenes by PCR (for primers, see Supplementary Table 1). Cultures were screened for mycoplasma contamination every 4 weeks.

Generation of midbrain dopamine neurons from opsin-expressing hESC lines

Induction of the ventral midbrain dopamine (mesDA) fate was induced as described previously[2] with the omission of FGF8. Briefly, neuralization was initiated 24 h after plating 1.5×10^5 hESCs/cm^2 (designated as day 0) onto Matrigel-coated plates (1:50, Life Technologies) by dual SMAD inhibition[46] using LDN193189 (100 nM, Stemgent) and SB431542 (10 μM, Tocris) in knockout serum replacement (KSR, Life Technologies) containing media. Ventralization was initiated by adding SHH C25II (100 ng/ml, R&D, days 1–6) and Purmorphamine (2 μM, Stemgent, days 1–6) as well as CHIR99021 (3 μM, Stemgent, days 3–12). From day 5 to day 10, knockout serum replacement (KSR) containing medium was replaced with N2 medium[46]. Media was changed to a 1:1 mixture of DMEM:F12 medium with N2 and Neurobasal medium with B27 (all Life Technologies) with CHIR (until day 13), ascorbic acid (0.2 mM, Sigma), brain-derived neurotrophic factor (BDNF, 20 ng/ml; R&D), glial cell line–derived neurotrophic factor (GDNF, 20 ng/ml; R&D), dibutyryl cAMP (0.2 mM; Sigma), transforming growth factor type β3 (TGFβ3, 1 ng/ml; R&D) and DAPT (5 μM; Tocris) on day 11. On day 20, cells were passaged by incubation with Accutase (Life Technologies) and replated (4×10^5 cells per cm^2) on dishes coated with polyornithine (PO; 15 μg/ml)/laminin (1 μg/ml)/fibronectin (2 μg/ml) in differentiation medium (DMEMF12/N2 and NB/B27 + ascorbic acid, BDNF, GDNF, dbcAMP, TGFβ3 and DAPT) and fed twice per week thereafter.

Calcium imaging

Transgene-expressing mesDA-rich cells were plated onto PO/laminin/fibronectin-coated 40-mm round glass coverslips in droplets of 5×10^4 cells/20 µl on day 30 and used for calcium imaging as described previously[47] between day 60 and day 100. Cultures were incubated with 5 µM Fura-2 (Life Technologies) for 30 min at 37 °C and then mounted in an FCS2 imaging chamber (Bioptechs). Cultures were perfused with normal Tyrodes's saline containing (in mM) NaCl 125, KCl 5, $CaCl_2$, $MgCl_2$, glucose 30, HEPES 25 and bovine serum albumin 0.1% w/v, pH 7.4 and supplemented with glutamate (50 or 100 µM) or KCl (55 mM, NaCl 75 mM). Cultures were imaged using a 40 × 1.3 numerical aperture oil immersion objective (Zeiss) every 5 s at 340 and 380 nm and illuminated repetitively for optogenetic testing for 15–120 s at 550 nm with light intensities ranging from 2–7.5 mW/mm^2 on an Axiovert 200 M Inverted Microscope (Zeiss) equipped with Metamorph Software (Molecular Devices) for ratiometric analysis. A minimum of three cultures from independent differentiations were analyzed for every experimental condition. Statistical analysis for ΔF/F between EYFP and HALO cultures in response to illumination was performed using unpaired two-tailed *t*-test. Error bars represent s.e.m.

HPLC

For dopamine measurement experiments, transgene-expressing cells were plated onto PO/laminin/fibronectin-coated 24-well plates in droplets of 2×10^5 cells (20 µl, 5 mm diameter) on day 30 and used between day 90 and day 100. HPLC with electrochemical detection (HPLC-EC) was done as previously described[36]. Briefly, before supernatant collection, cells were incubated in fresh DMEM:F12 + N2 media for 30 min. After exposure to either Tyrode's saline alone or supplemented with high KCl (55 mM, Sigma) or glutamate (100 µM, Sigma) for 10 min at room temperature and dim ambient light (approximately 300 lx), supernatant was collected and immediately mixed with perchloric acid (0.1 M final concentration) to deproteinize the sample and prevent dopamine auto-oxidation. For optogenetic inhibition, a 543-nm diode pumped solid-state pigtailed laser (OEM Laser) was used during secretagogue application at an output power of 100 mW to achieve an illumination of 4 mW/mm^2 over the entire culture area. Supernatant samples were sonicated at room temperature for 10 min, centrifuged at 10,000*g* for 5 min, stored at −80 °C and analyzed within the following 2 weeks by reversed phase HPLC-EC. The investigator performing HPLC measurements was blinded to sample identities. Cells in each sample were collected to normalize for protein content. DA concentrations in each group of samples were normalized to the levels in the corresponding control group; data are shown as averaged normalized values from five independent experiments. Statistical analysis was performed using one-way ANOVA and Sidak's multiple comparisons test (GraphPad Prism 6). Results are presented as mean ± s.e.m.

Animal procedures

All surgeries and behavioral tests were performed according to NIH guidelines and approved by the Institutional Animal Care and Use Committee (IACUC), the Institutional Biosafety Committee (IBC) and the Embryonic Stem Cell Research Committee (ESCRO). A total of 65 NOD-SCID IL2Rgc null mice (NSG, 20–30 g; Jackson Laboratory) were transplanted for

this study. Anesthesia was induced using ketamine (90 mg/kg; Akorn) and xylazine (4 mg/kg). For lesioning, 6-hydroxydopamine (6-OHDA, 10 μg, Sigma-Aldrich) was injected into the right striatum at the following coordinates (in millimeters from bregma): AP, +0.5; ML, +2.0; DV, −3.0 (from dura). Successfully lesioned mice (>6 amphetamine-induced rotations/min) were selected for transplantation and randomized to receive either HALO or EYFP transplants. 2×10^5 cells were resuspended in 2 μl of differentiation media and injected into the right striatum at the following coordinates (in mm from bregma): AP, +0.5; ML, +2.0; DV, −3.2 (from dura). Successfully recovered mice (an average of <2 amphetamine-induced rotations per min 16 weeks post-grafting) were selected for cannula implantation and optogenetic testing. Implantable optical fibers (numerical aperture 0.39, 200 μm core diameter, Thorlabs) were cut to a length of 2.5 mm, stereotactically inserted at the following coordinates (in mm from bregma): AP, +0.5; ML, +2.0; DV, −2.2 (from dura) and fixed on the skull with C&B-METABOND (Pearson Dental). Animals were allowed to recover from surgery for 48 h before the initiation of behavioral testing.

Tissue processing

Mice received pentobarbital (intraperitoneally 50 mg/kg) to induce deep anesthesia and were transcardially perfused with phosphate buffered saline and then 4% paraformaldehyde (PFA). Brains were extracted, post-fixed in 4% PFA and then soaked in 30% sucrose solutions for 1–5 days. They were sectioned on a cryostat after embedding in O.C.T. (Sakura-Finetek).

Immunohistochemistry

Cells were fixed in 4% PFA. Blocking solution for fixed cells and cryostat brain sections contained 5% FBS/0.1% NaN_3/0.3% Triton. Primary antibodies were diluted in 5% FBS/0.1% NaN_3/0.3% Triton and incubated overnight according to manufacturer recommendations (Supplementary Table 2). Secondary antibodies conjugated to Alexa488, Alexa555 or Alexa647 (Molecular Probes) were incubated for 4 h. Nuclear counterstain was visualized with 4′,6-diamidino-2-phenylindole (DAPI, Thermo Fisher).

Cell counting

For the determination of *in vitro* cell fates, 3 20× fields with a minimum of 500 cells were counted manually from three independent differentiation experiments. Data are presented as % of DAPI, TUJ or TH. For statistical comparison of HALO versus EYFP cell lines, unpaired two-tailed *t*-tests were performed assuming equal s.d. *In vivo* TH^+ neurons were counted and calculated using the optical fractionator workflow in Stereo Investigator software (Neurolucida) with representative grafts for the HALO group containing 8,775 and 6,750 TH^+ neurons, which is similar to our published results for hESC-based mesDA neuron grafts[2].

Behavioral assays

Amphetamine-induced rotations were assessed before transplantation as well as 8 and 16 weeks after transplantation. Animals with lesions only (+ sham graft) were included as negative controls alongside animals with EYFP and HALO grafts. Amphetamine-induced

rotations were recorded starting 10 min after intraperitoneal injection of d-amphetamine (10 mg/kg, Sigma) for 30 min. The data are presented as average number of rotations per minute.

The corridor test was performed as described previously[20,21]. Briefly, animals were food restricted (50% of regular intake, limited to 95% of initial body weight by IACUC) for 3 consecutive days and habituated to the corridor, including presentation of sucrose tablets in the corridor for 3 h on each of these days. Habituation and behavioral experiments were performed at approximately 300 lx dim indoor light. For optogenetic behavioral experiments animals were habituated to the corridor as described while being connected to the fiber optic cable but without the use of laser light. During optogenetic behavioral experiments a 543-nm diode pumped solid-state pigtailed laser (OEM Laser) was used to achieve a light power of >2 mW/mm^2 at a distance up to 1 mm from the tip of the fiber (http://www.stanford.edu/group/dlab/cgi-bin/graph/chart.php), which we calculated to cover more than 80% of the graft. The pigtailed laser was connected to the animal using a fiber optic rotary joint (Doric) to allow the animals to move and rotate freely in the corridor. Actual behavioral experiments were performed on days 4–6 after the initiation of food restriction. During the test animals were allowed to collect sucrose pellets from small cups (two pellets per cup) aligned to both sides of a narrow corridor for 5 min. Retrievals were scored separately from the right and left side of the animal; data are presented as fraction of retrievals from the side contra-lateral to the lesion over total retrievals. Nose pokes without retrievals or eating were not included in the analysis. Animals were deemed severely Parkinsonian when reaching a score of <0.15 with a minimum of at least four retrievals per 5-min session (average retrieval rate was 12 pellets/5 min). After behavioral testing, animals were returned to their home cage, provided with their daily feed and tested again the next day. R–(−)apomorphine (subcutaneously, 0.2 mg/kg, Sigma) was injected 20 min before the corridor trial. Apomorphine is a potent nonselective dopamine receptor agonist commonly used to assess dopaminergic function in the 6-OHDA lesion model, though at high concentration it can also exhibit antagonistic action on serotonergic and adrenergic receptor subtypes. All animals were subjected to the full corridor procedure including habituation and optogenetic testing twice, which resulted in consistent results between the two trials. Single data points in Fig. 3d represent averaged results from the two trials per animal. The investigator monitoring the live behavior was not blinded but the reliability of the live scoring was confirmed by two blinded investigators in posthoc analyses of video recordings of a subset of the behavioral sessions. Individual scores for all animals are presented in Supplementary Table 3. Statistical analysis was performed using the Kolmogorov-Smirnov normality test followed by one-way ANOVA and Sidak's multiple comparisons test (GraphPad Prism 6). Results are presented as mean ± s.e.m.

Electrophysiological recordings

Coronal striatal slices (250 μm thick) were prepared from adult mice using a vibratome (Leica VT1200) and ice-cold cutting solution containing (in mM): 100 glucose, 75 NaCl, 26 $NaHCO_3$, 2.5 KCl, 2 $MgCl_2$-$6H_2O$, 1.25 NaH_2PO_4-$6H_2O$ and 0.7 $CaCl_2$. Slices were allowed to recover in the solution for 30 min at 34 °C and then transferred to recording ACSF containing (in mM): 119 NaCl, 26.2 $NaHCO_3$, 10 glucose, 2.4 $CaCl_2$, 1.8 KCl, 1.2 $MgCl_2$-6 H_2O and 1.0 NaH_2PO_4-6 H_2O. The temperature for recordings was set at 32 °C

(±2 °C). For whole-cell patch clamp studies borosilicate glass pipettes with a tip resistance of 3–4 MΩ (G150F-4, Warner Instruments) were pulled on a P-97 Flaming-Brown micropipette puller (Sutter Instruments) and filled with: 115 mM K-gluconate, 20 mM KCl, 10 mM HEPES, 2 mM $MgCl_2$, 2 mM ATP-Mg, 2 mM ATP-Na_2 and 0.3 mM GTP-Na, (pH = 7.25, ~280 mOsm). For a subset of voltage-clamp studies, the pipette solution contained: 120 mM cesium-methanesulfonate, 11 mM glucose, 10 mM HEPES, 5 mM NaCl, 2 mM NaATP, 2 mM MgATP, 1.1 mM EGTA and 0.3 mM NaGTP (pH 7.3, 270–273 mOsm). Grafted human neurons expressing HALO or EYFP were visualized under a 40× water immersion objective by fluorescence and DIC optics (Olympus). Whole cell current clamp recording were performed with an Axopatch 200B amplifier (Molecular Devices) and digitized at 10 kHz with a Digidata 1332 or 1440A (Molecular Devices). Data were acquired using Clampex 10.2 software (Molecular Devices). In each cell, input resistance (measured by 100 pA, 100 ms duration hyperpolarizing pulses), resting membrane potential and spontaneous firing frequencies were monitored throughout the recording. Only grafted cells with a stable baseline activity for 5 min were analyzed for tonic firing. All drugs were from Sigma unless otherwise specified. For optogenetic inhibition, a 560-nm fluorescence lamp (Olympus) was used to achieve an illumination of 2 mW/mm^2.

For measuring host-to-graft synaptic integration, $EYFP^+$ dopamine neurons were voltage clamped at −60 mV. Excitatory post-synaptic currents were evoked by electrical stimulation (100–400 μA, 100 μsec duration) driven by an ISO-flex stimulus isolator (AMPI) and Master-8 pulse generator (AMPI). A concentric bipolar tungsten electrode (World Precision Instruments) was placed within 200 μm of the recording site. Stable baseline excitatory post-synaptic currents were obtained for 5 min before starting baseline recording in the presence of $GABA_A$ receptor antagonist picrotoxin (50 μM) and NBQX (10 μM) when indicated. Peak EPSC amplitudes were measured and sweeps were averaged for at least 5 min for each drug condition.

To examine the effect of the graft on striatal glutamatergic transmission, MSNs near the $EYFP^+$ graft core or adjacent to $EYFP^+$ processes were patch clamped and their input resistance and baseline resting membrane potential were monitored in the current clamp mode in the presence of $GABA_A$ receptor antagonist picrotoxin (50 μM). If series resistance changed by ±20% during the recording, data were discarded. Voltage-current relationships were measured by injecting step current from −300 to + 150 pA with +50 pA increments. The excitability and the rheobase of MSNs were measured by injecting step current from 0 to +150 pA with +10 pA increments. For the assessment of glutamatergic transmission onto MSNs, excitatory postsynaptic potentials (EPSPs) were evoked every 20 s by electrical stimulation of the corpus callosum using a bipolar tungsten electrode as described previously[48]. When indicated, the D1 receptor antagonist SCH39166 was used at a concentration of 2 μM. Data were analyzed in Clampfit (Molecular Devices) and after baseline correction EPSP values were reported as mean ± s.e.m. All experimental groups comprised a minimum of three animals. Statistical analysis was performed using the Kolmogorov–Smirnov normality test followed by one-way ANOVA and Sidak's multiple comparisons test (GraphPad Prism 6).

Fast-scan cyclic voltammetry (CV) recordings were performed with cylinder 5 μm carbon fiber electrodes (CFE) positioned at the dorsolateral striatum 50 μm below the exposed surface. Striatal slices were electrically stimulated at the corpus callosum using a bipolar stainless steel electrode. Square pulses of 0.4-ms duration were sent using an Iso-Flex stimulus isolator triggered by a Master-8 pulse generator (A.M.P.I.). Stimulus magnitude was selected by plotting a current–response curve and selecting the minimum value that produced the maximal response. Triangular voltage ramps from −450 mV holding potential to +800 mV over 8.5 ms (scan rate of 295 mV/ms) were applied to the CFE at 100-ms intervals. Current was recorded with an Axopatch 200B amplifier (Molecular Devices) filtered with 10-kHz low-pass Bessel filter and digitized at 25 kHz (ITC-18 board; InstruTech). Triangular wave generation and data acquisition were controlled by a locally written computer routine in IGOR Pro (WaveMetrics). Background-subtracted cyclic voltammograms obtained in dopamine solutions of known concentration served to calibrate the electrodes and to identify released dopamine.

Supplementary Material

Refer to Web version on PubMed Central for supplementary material.

Acknowledgments

We thank S. Oh and K. Manova (MSKCC molecular cytology core), and M. Tomishima (SKI stem cell core) for excellent technical support. We further thank Y. Schmitz (Sulzer laboratory) for advice on the corridor test. J.A.S. was supported by a Deutsche Forschungsgemeinschaft fellowship. The work was supported in part by US National Institutes of Health (NIH)/National Institute of Neurological Disorders and Stroke (NINDS) grant NS052671 and NYSTEM contract C028503 to L.S. and by the NINDS/NIH grant NS075222 to E.V.M.

This work was further supported by grants from the Parkinson's disease and Jeffry and Barbara Picower Foundations and the Udall Center of Excellence to D.S.

References

1. Kirkeby A, et al. Generation of regionally specified neural progenitors and functional neurons from human embryonic stem cells under defined conditions. Cell Reports. 2012; 1:703–714. [PubMed: 22813745]
2. Kriks S, et al. Dopamine neurons derived from human ES cells efficiently engraft in animal models of Parkinson's disease. Nature. 2011; 480:547–551. [PubMed: 22056989]
3. Roy NS, et al. Functional engraftment of human ES cell-derived dopaminergic neurons enriched by coculture with telomerase-immortalized midbrain astrocytes. Nat Med. 2006; 12:1259–1268. [PubMed: 17057709]
4. Tornero D, et al. Human induced pluripotent stem cell-derived cortical neurons integrate in stroke-injured cortex and improve functional recovery. Brain. 2013; 136:3561–3577. [PubMed: 24148272]
5. Dunnett SB, Hernandez TD, Summerfield A, Jones GH, Arbuthnott G. Graft-derived recovery from 6-OHDA lesions: specificity of ventral mesencephalic graft tissues. Exp Brain Res. 1988; 71:411–424. [PubMed: 2901978]
6. Kim JH, et al. Dopamine neurons derived from embryonic stem cells function in an animal model of Parkinson's disease. Nature. 2002; 418:50–56. [PubMed: 12077607]
7. Cummings BJ, et al. Human neural stem cells differentiate and promote locomotor recovery in spinal cord-injured mice. Proc Natl Acad Sci USA. 2005; 102:14069–14074. [PubMed: 16172374]
8. Gradinaru V, Thompson KR, Deisseroth K. eNpHR: a *Natronomonas halorhodopsin* enhanced for optogenetic applications. Brain Cell Biol. 2008; 36:129–139. [PubMed: 18677566]

9. Gradinaru V, et al. Molecular and cellular approaches for diversifying and extending optogenetics. Cell. 2010; 141:154–165. [PubMed: 20303157]
10. Chaudhury D, et al. Rapid regulation of depression-related behaviours by control of midbrain dopamine neurons. Nature. 2013; 493:532–536. [PubMed: 23235832]
11. Kravitz AV, et al. Regulation of parkinsonian motor behaviours by optogenetic control of basal ganglia circuitry. Nature. 2010; 466:622–626. [PubMed: 20613723]
12. Piña-Crespo JC, et al. High-frequency hippocampal oscillations activated by optogenetic stimulation of transplanted human ESC-derived neurons. J Neurosci. 2012; 32:15837–15842. [PubMed: 23136422]
13. Weick JP, et al. Functional control of transplantable human ESC-derived neurons via optogenetic targeting. Stem Cells. 2010; 28:2008–2016. [PubMed: 20827747]
14. Johnson MA, Weick JP, Pearce RA, Zhang SC. Functional neural development from human embryonic stem cells: accelerated synaptic activity via astrocyte coculture. J Neurosci. 2007; 27:3069–3077. [PubMed: 17376968]
15. Lindvall O, Kokaia Z. Stem cells in human neurodegenerative disorders–time for clinical translation? J Clin Invest. 2010; 120:29–40. [PubMed: 20051634]
16. Ganat YM, et al. Identification of embryonic stem cell-derived midbrain dopaminergic neurons for engraftment. J Clin Invest. 2012; 122:2928–2939. [PubMed: 22751106]
17. Miller JD, et al. Human iPSC-based modeling of late-onset disease via progerin-induced aging. Cell Stem Cell. 2013; 13:691–705. [PubMed: 24315443]
18. Guzman JN, Sanchez-Padilla J, Chan CS, Surmeier DJ. Robust pacemaking in substantia nigra dopaminergic neurons. J Neurosci. 2009; 29:11011–11019. [PubMed: 19726659]
19. Sørensen AT, et al. Functional properties and synaptic integration of genetically labelled dopaminergic neurons in intrastriatal grafts. Eur J Neurosci. 2005; 21:2793–2799. [PubMed: 15926926]
20. Dowd E, Monville C, Torres EM, Dunnett SB. The Corridor Task: a simple test of lateralised response selection sensitive to unilateral dopamine deafferentation and graft-derived dopamine replacement in the striatum. Brain Res Bull. 2005; 68:24–30. [PubMed: 16325001]
21. Grealish S, Mattsson B, Draxler P, Bjorklund A. Characterisation of behavioural and neurodegenerative changes induced by intranigral 6-hydroxydopamine lesions in a mouse model of Parkinson's disease. Eur J Neurosci. 2010; 31:2266–2278. [PubMed: 20529122]
22. Fujita S, et al. Apomorphine-induced modulation of neural activities in the ventrolateral striatum of rats. Synapse. 2013; 67:363–373. [PubMed: 23401143]
23. Kish LJ, Palmer MR, Gerhardt GA. Multiple single-unit recordings in the striatum of freely moving animals: effects of apomorphine and D-amphetamine in normal and unilateral 6-hydroxydopamine-lesioned rats. Brain Res. 1999; 833:58–70. [PubMed: 10375677]
24. Cenci MA, Kalen P, Mandel RJ, Wictorin K, Bjorklund A. Dopaminergic transplants normalize amphetamine- and apomorphine-induced Fos expression in the 6-hydroxydopamine-lesioned striatum. Neuroscience. 1992; 46:943–957. [PubMed: 1347413]
25. Rylander D, et al. Region-specific restoration of striatal synaptic plasticity by dopamine grafts in experimental parkinsonism. Proc Natl Acad Sci USA. 2013; 110:E4375–E4384. [PubMed: 24170862]
26. Nambu A. Seven problems on the basal ganglia. Curr Opin Neurobiol. 2008; 18:595–604. [PubMed: 19081243]
27. Surmeier DJ, Ding J, Day M, Wang Z, Shen W. D1 and D2 dopamine-receptor modulation of striatal glutamatergic signaling in striatal medium spiny neurons. Trends Neurosci. 2007; 30:228–235. [PubMed: 17408758]
28. Cepeda C, Buchwald NA, Levine MS. Neuromodulatory actions of dopamine in the neostriatum are dependent upon the excitatory amino acid receptor subtypes activated. Proc Natl Acad Sci USA. 1993; 90:9576–9580. [PubMed: 7692449]
29. Paillé V, et al. Distinct levels of dopamine denervation differentially alter striatal synaptic plasticity and NMDA receptor subunit composition. J Neurosci. 2010; 30:14182–14193. [PubMed: 20962239]

30. Steinbeck JA, Koch P, Derouiche A, Brustle O. Human embryonic stem cell-derived neurons establish region-specific, long-range projections in the adult brain. Cell Mol Life Sci. 2012; 69:461–470. [PubMed: 21779868]
31. Battista D, Ganat Y, El Maarouf A, Studer L, Rutishauser U. Enhancement of polysialic acid expression improves function of embryonic stem-derived dopamine neuron grafts in Parkinsonian mice. Stem Cells Transl Med. 2014; 3:108–113. [PubMed: 24311700]
32. Chan WS, et al. Differential expression of alpha-amino-3-hydroxy-5-methyl-4-isoxazole-propionate glutamate receptors in the rat striatum during postnatal development. Neurosignals. 2003; 12:302–309. [PubMed: 14739560]
33. Price CJ, Kim P, Raymond LA. D1 dopamine receptor-induced cyclic AMP-dependent protein kinase phosphorylation and potentiation of striatal glutamate receptors. J Neurochem. 1999; 73:2441–2446. [PubMed: 10582604]
34. Yan Z, et al. Protein phosphatase 1 modulation of neostriatal AMPA channels: regulation by DARPP-32 and spinophilin. Nat Neurosci. 1999; 2:13–17. [PubMed: 10195174]
35. André VM, et al. Dopamine modulation of excitatory currents in the striatum is dictated by the expression of D1 or D2 receptors and modified by endocannabinoids. Eur J Neurosci. 2010; 31:14–28. [PubMed: 20092552]
36. Pothos E, Desmond M, Sulzer D. L-3,4-dihydroxyphenylalanine increases the quantal size of exocytotic dopamine release *in vitro*. J Neurochem. 1996; 66:629–636. [PubMed: 8592133]
37. Snyder GL, et al. Regulation of phosphorylation of the GluR1 AMPA receptor in the neostriatum by dopamine and psychostimulants *in vivo*. J Neurosci. 2000; 20:4480–4488. [PubMed: 10844017]
38. Song RS, et al. ERK regulation of phosphodiesterase 4 enhances dopamine-stimulated AMPA receptor membrane insertion. Proc Natl Acad Sci USA. 2013; 110:15437–15442. [PubMed: 23986500]
39. Tukey DS, Ziff EB. Ca2+-permeable AMPA (alpha-amino-3-hydroxy-5-methyl-4-isoxazolepropionic acid) receptors and dopamine D1 receptors regulate GluA1 trafficking in striatal neurons. J Biol Chem. 2013; 288:35297–35306. [PubMed: 24133208]
40. Umemiya M, Raymond LA. Dopaminergic modulation of excitatory postsynaptic currents in rat neostriatal neurons. J Neurophysiol. 1997; 78:1248–1255. [PubMed: 9310416]
41. Bamford NS, et al. Repeated exposure to methamphetamine causes long-lasting presynaptic corticostriatal depression that is renormalized with drug readministration. Neuron. 2008; 58:89–103. [PubMed: 18400166]
42. Dell'Anno MT, et al. Remote control of induced dopaminergic neurons in parkinsonian rats. J Clin Invest. 2014; 124:3215–3229. [PubMed: 24937431]
43. Dull T, et al. A third-generation lentivirus vector with a conditional packaging system. J Virol. 1998; 72:8463–8471. [PubMed: 9765382]
44. Kim H, et al. miR-371-3 expression predicts neural differentiation propensity in human pluripotent stem cells. Cell Stem Cell. 2011; 8:695–706. [PubMed: 21624813]
45. Watanabe K, et al. A ROCK inhibitor permits survival of dissociated human embryonic stem cells. Nat Biotechnol. 2007; 25:681–686. [PubMed: 17529971]
46. Chambers SM, et al. Highly efficient neural conversion of human ES and iPS cells by dual inhibition of SMAD signaling. Nat Biotechnol. 2009; 27:275–280. [PubMed: 19252484]
47. Barreto-Chang OL, Dolmetsch RE. Calcium imaging of cortical neurons using Fura-2 AM. J Vis Exp. 2009
48. Akopian G, Walsh JP. Corticostriatal paired-pulse potentiation produced by voltage-dependent activation of NMDA receptors and L-type Ca(2+) channels. J Neurophysiol. 2002; 87:157–165. [PubMed: 11784738]

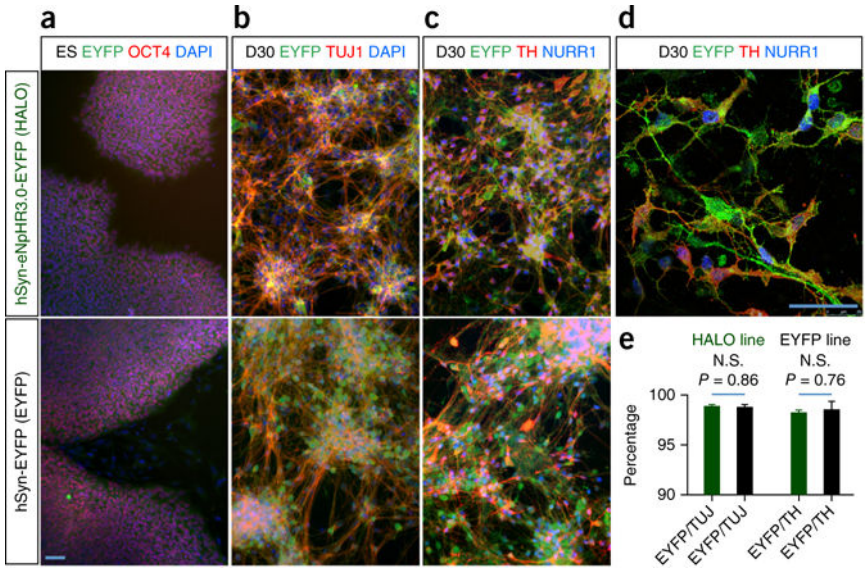

Figure 1.

In vitro immunocytochemical characterization of opsin-expressing hESC lines and dopaminergic progeny. Upper panels, hSyn-eNpHR3.0-EYFP (HALO) line, lower panels, hSyn-EYFP (EYFP) line. (**a**) Transgene harboring clonal hESC lines expressed OCT4 (red). (**b**) By day (D) 30, >98% of all TUJ^+ neurons (red) expressed HALO/EYFP. (**c**) At D30, >98% of all TH^+ (red)/$NURR1^+$ (blue) neurons expressed HALO/EYFP. (**d**) Confocal imaging shows HALO localization in TH^+/$NURR1^+$ neurons largely confined to membranes and processes. (**e**) Quantification and comparison of transgene expression in all neurons (t = 0.18, P = 0.86, N.S.) and TH^+ neurons (t = 0.32, P = 0.76, N.S.) between the HALO and EYFP line. Scale bar, 50 μm. Error bars represent s.e.m.

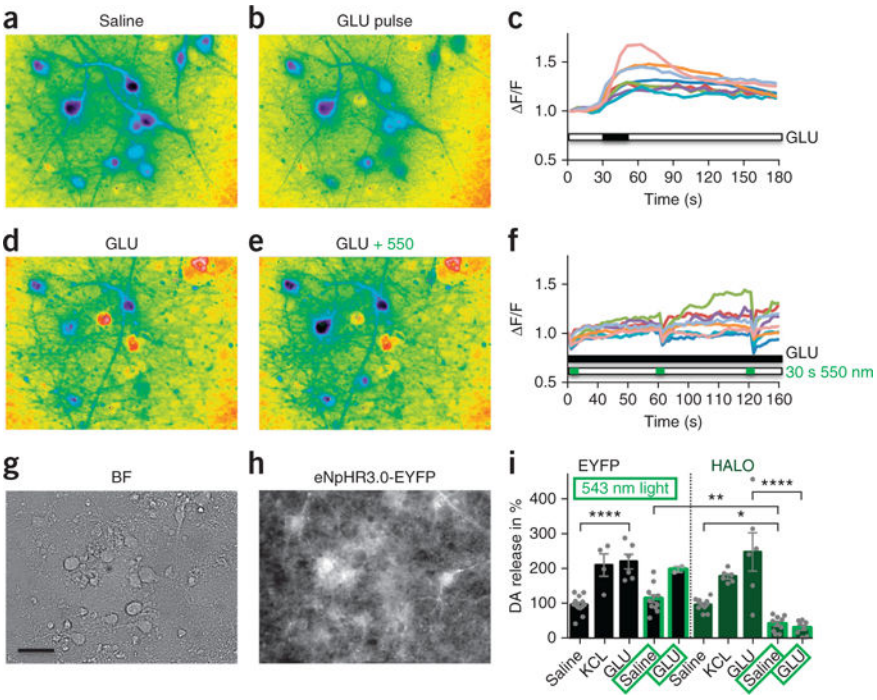

Figure 2.

In vitro physiologic and neurochemical assessment of optogenetic control. (**a**) Representative ratiometric image of a D90, HALO-expressing, mesDA-rich culture after incubation with Fura-2. (**b,c**) A glutamate pulse (GLU, 100 μM) generates a calcium response (**b**), quantified in **c**. (**d–f**) During continuous glutamate perfusion (GLU, 50 μM, d) 550-nm light pulses (**e**) generate inactivating calcium signals in soma and dendrites of neurons, quantified in **f**. (**g,h**) Bright-field (**g**) and eNpHR3.0-EYFP expression (**h**) of the same region. Scale bar, 20 μm. (**i**) HPLC measurements of dopamine (DA) release from 90- to 100-day-old cultures after exposure to various stimuli and in the presence or absence of light-induced neuronal silencing. KCl (55 mM) and glutamate (GLU, 100 μM) exposure increase dopamine release in both EYFP- (black bars) and HALO- (green bars) expressing dopamine neurons by about twofold. Optogenetic inhibition at 543 nm (bars with bright green border) reduced dopamine release from HALO-expressing cultures only, in the presence and absence of glutamate stimulation. $^{*}P < 0.05$, $^{**}P < 0.01$, $^{****}P < 0.0001$.

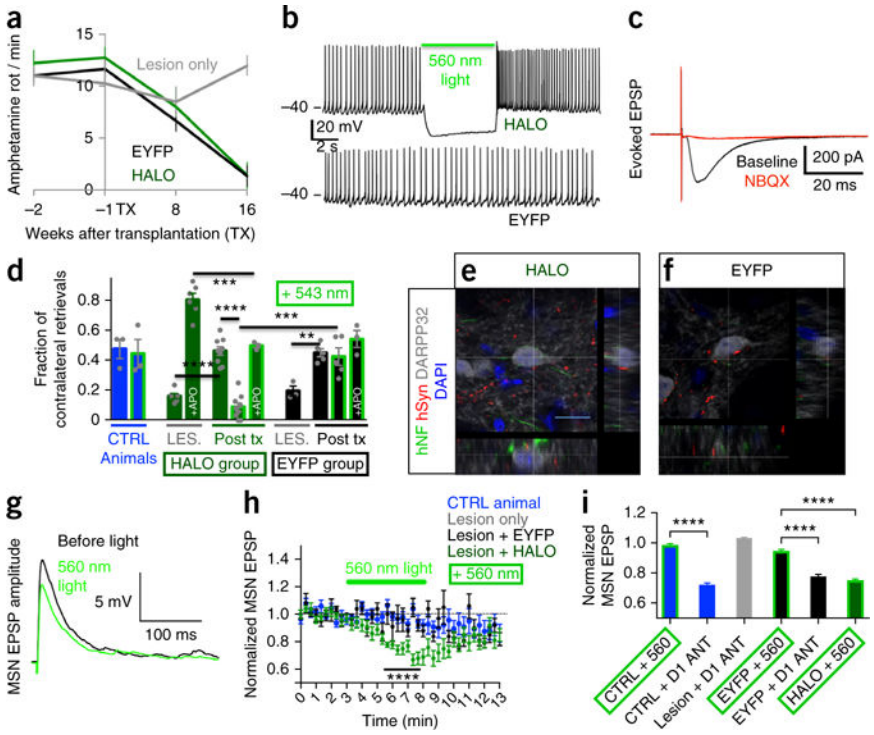

Figure 3.

Behavioral, physiological and morphological assessment of graft functional connectivity. (**a**) Amphetamine-induced rotation assay demonstrates behavioral recovery of grafted animals. (**b**) Characteristic ~3-Hz pacemaking activity is optogenetically silenced in HALO-expressing neurons only. (**c**) Evoked postsynaptic potentials (EPSPs) in grafted HALO-expressing neurons following local electrical stimulation are blocked by AMPA-receptor-antagonist NBQX. (**d**) In the corridor test, unlesioned and nongrafted animals (CTRL, blue bars) did not show lateralized behavior regardless of illumination (green border). Before transplantation, lesioned animals (LES.) showed a strong preference for food retrieval on the side ipsilateral to the lesion, which was inverted by the dopamine agonist apomorphine (LES. + APO, green bar). Animals with EYFP grafts (black bars POST TX) recovered from lesion-induced motor deficiency and were insensitive to illumination or apomorphine. Animals with HALO grafts (green bars POST TX) also recovered from the lesion but reverted to lateralized behavior during optogenetic graft silencing, which was reversed by prior apomorphine injection. Significance was calculated using one-way ANOVA ($F(10, 44) = 29.99$, $P < 0.0001$). Adjusted P values indicated in the graph are calculated using Sidak's multiple comparisons test. (**e,f**) Confocal analysis of human axons staining for human neurofilament (hNF) and human synaptophysin (hSyn) extend from HALO and EYFP grafts into the host striatum and are in close contact with host DARPP32^{+} MSNs. Scale bar, 10 μm. (**g**) Representative examples of electrically evoked AMPA EPSPs recorded from a MSN before and during optogenetic graft silencing in a HALO animal. (**h**) EPSP amplitudes in MSNs were modulated by optogenetic inhibition of HALO- but not EYFP-expressing grafted neurons or in CTRL animals. (**i**) EPSPs recorded from MSNs in CTRL, lesioned,

EYFP or HALO striata in the presence of optogenetic graft silencing or D1 receptor blockade with 2 μM SCH39166. $^{**}P < 0.01$, $^{***}P < 0.001$, $^{****}P < 0.0001$.